Deep Learning for Ocean Remote Sensing: An Application of Convolutional Neural Networks for Super-Resolution on Satellite-Derived SST Data

Aurélien Ducournau*, Ronan Fablet*
*Institut Mines-Télécom, Télécom-Bretagne; UMR 6285 LabSTICC, Brest, France
Email: {aurelien.ducournau, ronan.fablet}@telecom-bretagne.eu

***Abstract*—In this paper, we propose to address the downscaling of ocean remote sensing data using image super-resolution models based on deep learning, and more particularly Convolutional Neural Networks (CNNs). The goal of this study, for which we focus on satellite-derived Sea Surface Temperature (SST) data, is to evaluate the efficiency and the relevance of deep learning architectures applied to oceanographic remote sensing data. By using a CNN architecture, namely SRCNN (Super Resolution CNN), on a large-scale dataset of SST fields, we show that it allows a considerable gain in terms of PSNR compared to classical downscaling techniques. These results point out the relevance of deep learning models specifically trained for ocean remote sensing data and advocate for other applications to the reconstruction of high-resolution sea surface geophysical fields from multi-sensor satellite observations.**

***Index Terms*—Deep Learning, Convolutional Neural Networks, Ocean Remote Sensing Data, Super-Resolution.**

I. Introduction

In the last two decades, multi-satellite and multi-sensor measurements of sea surface parameters, such as sea surface temperature (SST), sea surface height (SSH), ocean colour, sea surface salinity (SSS), ... have provided a wealth of information about ocean circulation and atmosphere-ocean interactions. The availability of such large-scale satellite-derived observation datasets has also raised the interest of the scientific community towards data-driven analyses besides classical model-driven schemes. As a peculiar example, one may cite the emergence of analog schemes for a variety of reconstruction and forecasting issues: high-resolution wind field downscaling [1], [2], atmospheric corrections [3], missing data interpolation [4], [5], ...

In the present paper, we focus on downscaling issues on SST fields. The state-of-the-art approaches may be categorized mainly according to EOF-based approaches [1], [4], analog schemes [5] and other machine learning models, especially kernel methods [2] and neural networks [3]. Downscaling is the problem of reconstructing a high-resolution (HR) observation from a low-resolution (LR) one. In the case of 2D fields, this problem refers to image super-resolution [6] in the computer vision and pattern recognition community. Apart from traditional early interpolation techniques, the most recent approaches for image super-resolution rely on example-based strategies [7] to learn the underlying transformation between low and high resolution images. Different learning approaches include statistical image priors [8], internal patch similarities in the same image [9], [10], or learning mapping functions from external low and high-resolution patches [11], [12] in particular with sparse coding [13]–[15]. Recently, deep learning has emerged as the state-of-the-art approach for image super-resolution [16]–[18] and applications to other image reconstruction problems (e.g., image denoising and inpainting [19], texture synthesis [20]) are also rapidly developing. One of the key features of deep learning is its ability to train complex models from large-scale ground-truth datasets, while controlling the computational efficiency of these models.

Given the availability of such large-scale datasets for ocean remote sensing, it appears very timely to investigate the potential of deep learning models for reconstruction issues from satellite-derived observations. Some questions naturally arise: do deep learning models reach state-of-the-art performance for ocean remote sensing datasets? Do deep learning models trained for natural images apply to ocean remote sensing data? Does the large-scale space-time variability of ocean dynamics affect learning efficiency? What are the relevant parameters of deep models for ocean remote sensing data?

This paper aims at addressing these questions through a specific case-study: the reconstruction of high-resolution SST fields from a low-resolution observation. Using as ground-truth dataset a high-resolution cloud-free gridded product, namely OSTIA [21], we benchmark different parameterizations of a deep learning architecture [16] and discuss their relevance. The subsequent is organized as follows. Section II describes the considered deep learning model for super-resolution [16]. Section III presents the considered experimental setting and the associated results. We further discuss the key contributions of this study in Section IV.

II. Convolutional Neural Networks (CNNs) for image super-resolution

A. Deep learning and CNNs

Deep learning [22] arises from concepts of machine learning and especially neural networks, which goal is to estimate different kinds of functions that can depend on a large number of inputs. In traditional "shallow" machine learning, we usually compute higher-level representations of the data before training classifiers (SVMs, Random Forests, ...). These representations are hand-crafted and require a certain amount of

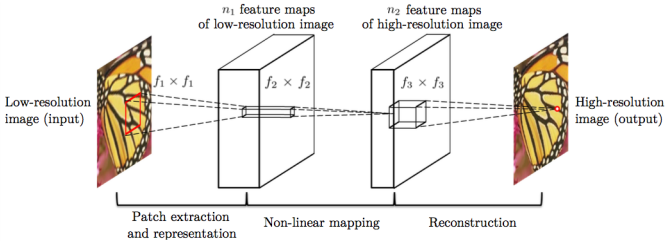

Fig. 1. Given a LR image, the first layer of the SRCNN extracts a set of feature maps. The second layers maps these features maps nonlinearly to HR patches representations. The last layer combines the predictions within a spatial neighborhood to produce the final HR image. Image taken from [16].

engineering. In comparison, deep learning approaches attempt to learn a set of representations directly from the data through a hierarchical unsupervised feature learning. This process involves a deep architecture, organized in inter-connected layers (the output of each layer is connected to the next layer's input) of transformation units that are able to automatically extract prominent high-level features from the data.

In many computer vision and pattern recognition approaches, the most popular deep learning architectures are based on Convolutional Neural Networks (CNNs), which use convolution filters as their main transformation units. Each layer of a CNN consists of a set of convolution filters of the same size connected to the previous and next layers, such that the output of a given filter of layer L is a function of outputs of filters of layer $L-1$. This hierarchy allows to learn sets of features with different levels of abstraction, the last layers learning the higher-level features. The weights of the filters constitute the model being learned through an optimization process that involves the minimization of the error between the output produced by the overall network and the ground-truth output. The use of convolutional layers is highly popular in computer vision, because it exploits the stationarity property of natural images. It means that in natural images, we can observe patterns that may repeat in different parts of a given image. The convolution can capture these patterns and learn accurate prominent features from them. Another key feature of CNNs is the need of a large-scale dataset in order for the network to learn a model that is complex enough to encapsulate a wide variety of features. Given the availability of such large-scale datasets for ocean remote sensing, it makes sense to investigate deep learning approaches for this kind of data. We refer the reader to [22] for an in-depth description of CNNs.

B. Super-Resolution CNN (SRCNN)

Few architectures have been proposed very recently for super-resolution [16]–[18], so it is difficult to draw a panel of standard methods for this application. However, among them the Super Resolution CNN (SRCNN) has emerged as a robust baseline and outperformed the most recent image super-resolution approaches [16]. In addition, its rather simplicity and easiness of use makes it the best choice to investigate the relevance of deep learning for new kinds of data such as SST.

The SRCNN takes as output the HR image, since this is what we want to predict from the LR observation. The latter (obtained directly or following a downscaling of the original HR image) is first resized to fit the HR image (with a traditional bicubic interpolation) and serves as the input of the network. The goal of the training phase is to learn the weights of the different filters of the network that will transform the bicubic reconstructed LR into the HR image, by minimizing the error between the output produced by the network and the original HR image. The SRCNN (illustrated in Fig. 1) consists of three layers of convolution filters, described below:

1) **Patch extraction and representation:** The first layer acts as a feature extractor, by densely extracting patches from the LR image and computing high-level representations from them. For a given LR image Y, its output $F_1(Y)$ is given by:

$$F_1(Y) = \max(0, W_1 * Y + B_1), \tag{1}$$

where $*$ is the convolution operator, W_1 and B_1 represent respectively the weights and biases of the filters.

2) **Non-linear mapping:** The second layer nonlinearly maps each vector onto another one, which corresponds to the representation of the same patch from the reconstructed HR image. Its output $F_2(Y)$ is given by:

$$F_2(Y) = \max(0, W_2 * F_1(Y) + B_2). \tag{2}$$

3) **Reconstruction:** The third and final layer aggregates the high-resolution patch-wise representations to generate the final HR image. Its output (and the output of the network) $F_3(Y)$ is given by:

$$F_3(Y) = W_3 * F_2(Y) + B_3. \tag{3}$$

During training, the network is fed with small HR image patches extracted from the training data, along with their resized LR counterpart. To avoid border effects, the LR patch is taken as the center sub-image of the resized LR patch and is consequently of a smaller size depending on the filter sizes. The model is optimized by traditional stochastic gradient descend [22] minimizing the Mean Squared Error (MSE) between the HR output $F_3(Y_i)$ produced by the network and the original HR. For the reconstruction, the entire LR image is simply convoluted, layer by layer, with the different filters of the network that have been learned during training.

III. Experiments

In this section, we apply the SRCNN described in the previous section to the reconstruction of LR SST fields. We first describe our experimental setting and then give quantitative results of our application.

A. Experimental setting

Dataset: As case-study application, we consider OSTIA SST time series from January 2007 to April 2016. OSTIA product is delivered daily by UK Met Office [21] with a $0.05°$ spatial resolution (approx. 5km). The OSTIA analysis combines satellite data provided by infrared sensors (AVHRR,

AATSR, SEVIRI), microwave sensors (AMSRE, TMI) and in situ data from drifting and moored buoys. OSTIA SST time series provide a representative ground-truth dataset to mimic the reconstruction of a HR SST field from a LR observation, as provided by microwave sensors [21].

Benchmarked models: We consider 2 parameterizations of the SRCNN architecture [16] using a filter size of 1 and 3 respectively in the second layer of the network, because it has been highlighted [16] as the parameter that influences the most the reconstruction. Other parameters remain unchanged: 64 filters of size 9×9 in the first layer, 32 filters in the second layer and one 5×5 filter in the third layer. The models are trained for the reconstruction of the full HR SST field (referred hereafter as "Full field") or of the difference between the HR SST field and the bicubic interpolation of the LR field (referred hereafter as "Detail field"). All SRCNN models use 33×33 image patches for the input layer, and 21×21 or 19×19 ones for the output layer for a filter size of 1 or 3 respectively. For comparison purposes, we also include in our evaluation a linear EOF-based downscaling model [1], [2].

Training setting: We consider different training strategies for the SRCNN models. We compare the original SRCNN model trained from ImageNet dataset [23] to models trained from SST data. In this respect, we aim at evaluating whether or not region-specific models are more relevant. To this end, a highly-dynamic region off South Africa (10.025°W-34.925°E, 35.975°S-65.925°S), which involves complex fine-scale SST structures, is selected as reference local region in our analysis. 500 different SST fields have been randomly selected as training set. For a given SRCNN architecture, we train a local model using all overlapping patches (with a stride of 14 pixels) of the reference region for every SST field of the training set, resulting in approximately 300 000 patches. We also train a global model using the same number of patches randomly sampled over the global ocean surface and the whole training set. For those training procedures, we use a random initialization of CNN weights and 5-million training iterations. We also evaluate a fine-tuned version of the local model, i.e. a local model trained from an initialization provided by the global model. Only 500 000 training iterations are performed for fine-tuning. In all cases, prior to training, the considered SST patch datasets are normalized between 0 and 1 as requested by CNN architecture. All the CNN tests are performed with Caffe library [24].

Evaluation setting: For any model, we evaluate its performance in terms of the PSNR between the original HR image and the reconstructed one:

$$PNSR = 10.\log_{10}\left(\frac{1}{\sum_{i=1}^{n} |I(i) - \hat{I}(i)|^2/n}\right), \qquad (4)$$

where I denotes the original HR image, $\hat{I}$ is the reconstructed image and n the number of pixels in the image. $|I(i)-\hat{I}(i)|$ are the residuals, i.e. the difference between the reconstruction and the original HR image. We also evaluate the PSNR gain with respect to the baseline bicubic interpolation, i.e. $PSNR_{gain} = PSNR_{alg} - PSNR_{bicubic}$ for a given algorithm alg. For each model, we evaluate the PSNR gain for an independent test SST dataset (not taken in the training set) both for the global ocean and the reference region. For the global ocean, we consider randomly sampled regions (the same size as the reference region) from the whole ocean surface of the test dataset. Beyond the global PSNR, we further analyze reconstruction with respect to local image features, especially the gradient magnitude as super-resolution models are mainly expected to affect areas depicting large gradient magnitudes.

TABLE I

MEAN PSNR GAIN COMPARED TO THE BICUBIC INTERPOLATION FOR MULTIPLE MODELS. SCALE BETWEEN HR AND LR SST FIELDS IS EQUAL TO 3. FILTERS OF SIZE 1 AND 3 HAVE BEEN USED FOR THE SECOND LAYER OF THE SRCNN. GLOBAL, LOCAL AND FINE-TUNED MODELS HAVE BEEN EVALUATED FOR A REFERENCE OR A RANDOM REGION.

Model	Reference region	Random region
Detail field		
1x1 filters, global model	3.57 ± 0.78	3.35 ± 0.80
1x1 filters, local model	3.78 ± 0.75	3.28 ± 0.85
1x1 filters, fine-tuned model	3.84 ± 0.78	3.42 ± 0.86
3x3 filters, global model	4.30 ± 0.88	3.99 ± 0.90
3x3 filters, local model	4.49 ± 0.90	3.88 ± 0.84
3x3 filters, fine-tuned model	4.48 ± 0.85	3.92 ± 0.93
Full field		
3x3 filters, local model	1.18 ± 0.67	0.95 ± 0.96
SRCNN ImageNet [16]	0.77 ± 1.51	1.31 ± 0.73

B. Experimental results

We report in Tab. I the reconstruction performance, in terms of mean PNSR gain, of the different models tested in our experiments, for a scale of 3 between HR and LR SST fields. Overall, all SRCNN models show significant improvement w.r.t. the bicubic interpolation, with PNSR gains ranging from 0.8 to 4.5. It might be noted that the latter is consistent with the values reported for natural images [7], [16]. SRCNN models for the full SST field are greatly outperformed by models targeted at the detail field. This probably relates to the space-variability of mean SST value within each SST patch. SST field depicts clear latitudinal large-scale as well as seasonal variabilities. Learning models for the detail field allows us to get rid of these variabilities and resorting to more stationary data, which is an important prerequisite for the efficiency of CNN models. Though the advantage of learning differences between HR and LR has also been reported for natural images [15]. The large-scale space-time variabilities of SST fields are also regarded as a key factor to explain that the SRCNN model trained with natural images [16] leads to lower reconstruction performance, with a difference of more than 3.5dB w.r.t. the best SRCNN model. This result particularly emphasizes the need to train domain-specific models for ocean remote sensing data.

From a further analysis of the performance of the SRCNN models for the detail field, two main conclusions can be drawn. On one hand, the more complex the model (i.e. in our case the filter size in one given layer), the more accurate the reconstruction with a PNSR gain up to 0.9 dB using a filter size of 3

rather than 1 in the second layer of the network. On the other hand, and more importantly for the considered application field, models trained specifically for the considered reference region leads to a PSNR gain of about 0.2dB compared to a model trained globally. Conversely, the local model may still be valid for an application to the global ocean at the expense of mean PSNR loss of $\sim 0.1/0.2$ dB compared to a model trained globally. Interestingly, the fine-tuned model, *i.e.* a model trained locally from an initialization given by the global model and using 10 times less training iterations, resorts to the same reconstruction performance than the local model trained from scratch (respectively 4.48 and 4.49 of mean PSNR gain for the reference region). These results suggest that all models share some convolutional patterns that are not domain-specific, whereas some parameters, especially for the second layer of the network, may be expected to depict a greater space-time variability.

In the following, we further characterize the reconstruction performance of the proposed SRCNN models. We focus on the local model learned with 3×3 filters in the second layer of the SRCNN architecture, since it provides the best results in Tab. I. In Fig. 2, we examine the residuals distribution for two examples of super-resolution of SST fields, including a comparison between the best SRCNN model and the bicubic interpolation. The examples refer to one of the lowest PSNR gains of the considered time series (i.e. 3.39), and the second one to one of the highest PSNR gains (i.e. 5.24). Obviously, as illustrated by the distribution of error residuals, the improvement is more noticeable for the second case, which also corresponds to the highest gradient magnitude over the whole field. These two examples point out that the largest gains from the bicubic interpolation occurs along high SST gradient structures. To further illustrate this, we report the mean (over the whole validation dataset) PSNR gain as a function of the original high-resolution gradient magnitude percentiles in Fig. 3. These results clearly emphasize that the SRCNN model enhances strong spatial variations which are poorly resolved by the bicubic interpolation. A visual example of the SST field reconstructions is given in Fig. 4. By looking only at the original and reconstructed SST fields (Fig. 4.a-c), it is difficult to see a clear difference between SRCNN and bicubic reconstructions, even if the latter may seem smoothed compared to the original, as the SRCNN may look closer to the original field. By looking at the gradient magnitudes (Fig. 4.d-f), it is clearer that the SRCNN reconstruction is able to enhance the gradients that have been smoothed out by the bicubic interpolation. Fig. 4.g-h shows the residuals of the bicubic and SRCNN reconstructions, and Fig. 4.i the residuals gain between bicubic and SRCNN reconstruction. We can clearly see the error reduction induced by the SRCNN. Interestingly, we can observe that the strongest residuals (for bicubic interpolation) occur in the regions of strongest gradient, as well as the strongest gains between SRCNN and bicubic reconstructions. These results once again emphasize that, as expected, the SRCNN models are mainly affecting areas depicting large gradient magnitudes.

TABLE II
MEAN PSNR VALUES OF SST RECONSTRUCTION FOR DIFFERENT SCALES BETWEEN HR AND LR AND DIFFERENT RECONSTRUCTION APPROACHES.

Scale	Bicubic	EOF-Linear [1]	EOF-SVR [2]	SRCNN
2	43.54	46.25	46.72	**47.31**
3	35.17	38.63	39.11	**39.66**
4	29.67	32.68	32.81	**34.02**

Finally, we compare the reconstruction performance of the SRCNN approach to two standard EOF ones, namely Linear-EOF [1] and SVR-EOF [2]. These approaches first perform an EOF (Empirical Orthogonal Functions) transformation of the whole LR field, which will be used to learn a regression model for each HR grid point in the field, using respectively linear [1] and Support Vector Regression (SVR) [2]. Tab. II reports the mean PSNR values for the reconstruction obtained with the three approaches, as well as the bicubic interpolation. One can see that SRCNN clearly outperforms the two EOF methods, which represent the baseline in geophysical reconstruction. In addition, deep learning models tend to be much more adaptive, since the need to learn a different model for each grid point in EOF-based approaches makes them naturally local and impossible to apply to another local region. On the contrary, results in Tab. I show that even models built locally can apply successfully to random regions, and can be suitable at a global scope. Overall, these results show that deep learning approaches display a great potential for ocean remote sensing applications, and may be investigated further.

IV. DISCUSSION

This study addresses the application of deep learning to ocean remote sensing data. While deep learning has rapidly become the state-of-the-art framework for a variety of problems in pattern recognition and computer vision, its applicability to remote sensing data, and more specifically ocean remote sensing, remains to be investigated. Whereas recent studies have mainly focused on hand-crafted machine learning techniques, especially for downscaling issues [2], the availability of large-scale remote sensing datasets makes deep learning architectures increasingly appealing, as their success in the pattern recognition field strongly relates to the use of such large-scale training datasets. As case-study, we consider the reconstruction of high-resolution (HR) SST fields from low-resolution (LR) observations and investigate different parameterizations of a convolutional neural network (SRCNN) [16].

Our experiments clearly points out the relevance of CNNs for the considered dataset with clear improvement over the bicubic interpolation, and also over traditional state-of-the-art approaches for geophysical fields downscaling. We can also draw a number of conclusions of interest:

- Given the large-scale space-time variabilities embedded in global satellite-derived geophysical fields, deep learning architectures should be applied to detail or anomaly field to reach significant reconstruction performance;
- Fine-tuned region-specific models, initialized from a global model, provide the best trade-off between train-

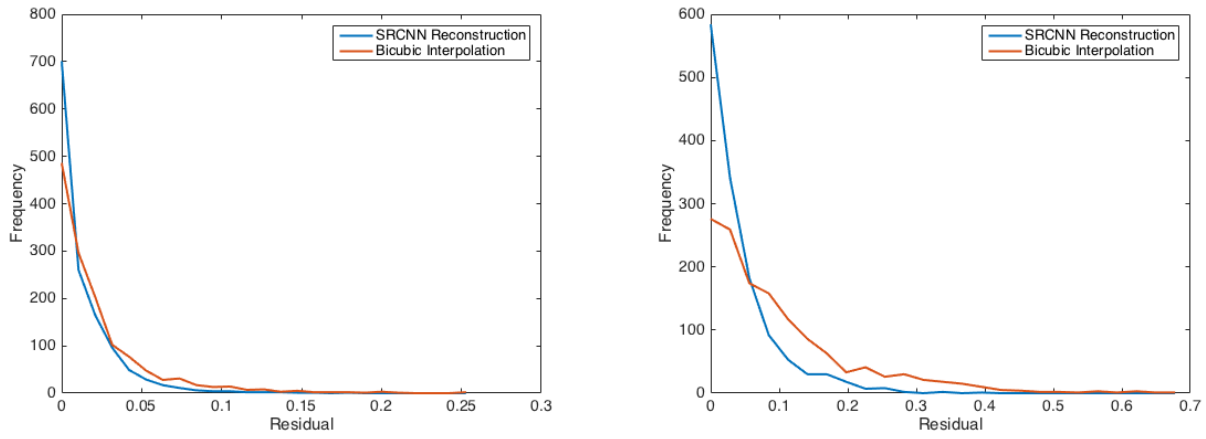

Low gradient (3.39 PSNR gain) Strong gradient (5.24 PSNR gain)

Fig. 2. Residuals distribution over the SST field for the reconstructed SRCNN and bicubic interpolation, shown for the 1% of highest gradient magnitude. Left: SST field with low gradient (mean of 2.59 and std of 0.36). Right: SST field with strong gradient (mean of 4.55 and std of 1.22).

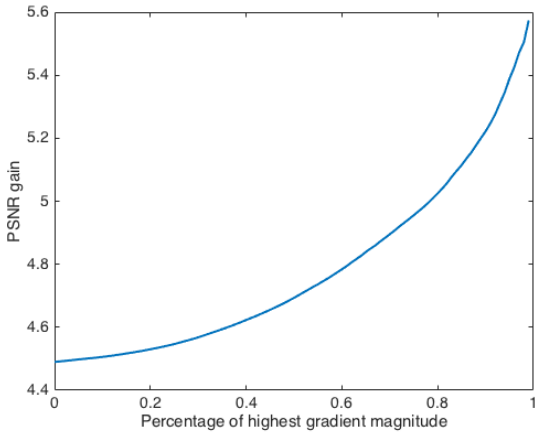

Fig. 3. Mean PSNR gain by considering only locations where gradient magnitude is above a given percentage.

ing computational complexity and reconstruction performance. Besides, compared to hand-crafted models, *e.g.* [2], deep architectures provide additional flexibility to balance between global for low-level network layers (here, the first and third layer of the SRCNN) and region-specific parameterizations for higher-level network layers (here, the second layer of the SRCNN);

- Trained convolutional models act as customized contrast enhancement models, which enhance high-gradient structures (filaments, fronts,...) smoothed out by the interpolation of the low-resolution observation. As such, it may be regarded as a new means to investigate inter-scale relationships, especially mesoscale-to-submesoscale cascade from satellite-derived ocean remote sensing data.

This study opens a variety of research avenues to further investigate new deep learning-based models for the reconstruction of geophysical dynamics from satellite-derived remote sensing data. Beyond application to other geophysical fields, e.g. sea surface fields (sea surface height and salinity, ocean colour, wind fields), the exploration and analysis of ocean-dynamics-specific, including multi-tracer model, seems particularly appealing along with the exploitation of the different observation sampling geometry (e.g., 2D fields, cloud-induced missing data, time series, narrow-swath satellite data, ...). Further work will also include the comparison of deep learning techniques with state-of-the-art methods for typical image super-resolution, and the design of new CNNs architectures.

REFERENCES

[1] K. Goubanova, V. Echevin, B. Dewitte, F. Codron, K. Takahashi, P. Terray, and M. Vrac, "Statistical downscaling of sea-surface wind over the Peru-Chile upwelling region: diagnosing the impact of climate change from the IPSL-CM4 model," *Climate Dynamics*, vol. 36, no. 7-8, pp. 1365–1378, May 2010.

[2] L. He, R. Fablet, B. Chapron, and J. Tournadre, "Learning-Based Emulation of Sea Surface Wind Fields From Numerical Model Outputs and SAR Data," *IEEE Journal of Selected Topics in Applied Earth Observations and Remote Sensing*, vol. 8, no. 10, pp. 4742–4750, Oct. 2015.

[3] J. Brajard, C. Moulin, and S. Thiria, "Atmospheric correction of SeaWiFS ocean color imagery in the presence of absorbing aerosols off the Indian coast using a neuro-variational method," *Geophysical Research Letters*, vol. 35, p. 20604, Oct. 2008.

[4] A. Alvera Azcarate, A. Barth, D. Sirjacobs, F. Lenartz, and J.-M. Beckers, "Data Interpolating Empirical Orthogonal Functions (DINEOF): a tool for geophysical data analyses," *Mediterranean Marine Science*, vol. 12, no. 3, 2011.

[5] R. Fablet and F. Rousseau, "Joint Interpolation of Multisensor Sea Surface Temperature Fields Using Nonlocal and Statistical Priors," *IEEE Journal of Selected Topics in Applied Earth Observations and Remote Sensing*, vol. 9, no. 6, pp. 2665–2675, Jun. 2016.

[6] C.-Y. Yang, C. Ma, and M.-H. Yang, "Single-Image Super-Resolution: A Benchmark," in *Computer Vision ECCV 2014*, ser. Lecture Notes in Computer Science. Springer International Publishing, Sep. 2014, no. 8692, pp. 372–386.

[7] R. Timofte, R. Rothe, and L. Van Gool, "Seven ways to improve example-based single image super resolution," in *2016 IEEE Conference on Computer Vision and Pattern Recognition*, Jun. 2016, arXiv: 1511.02228.

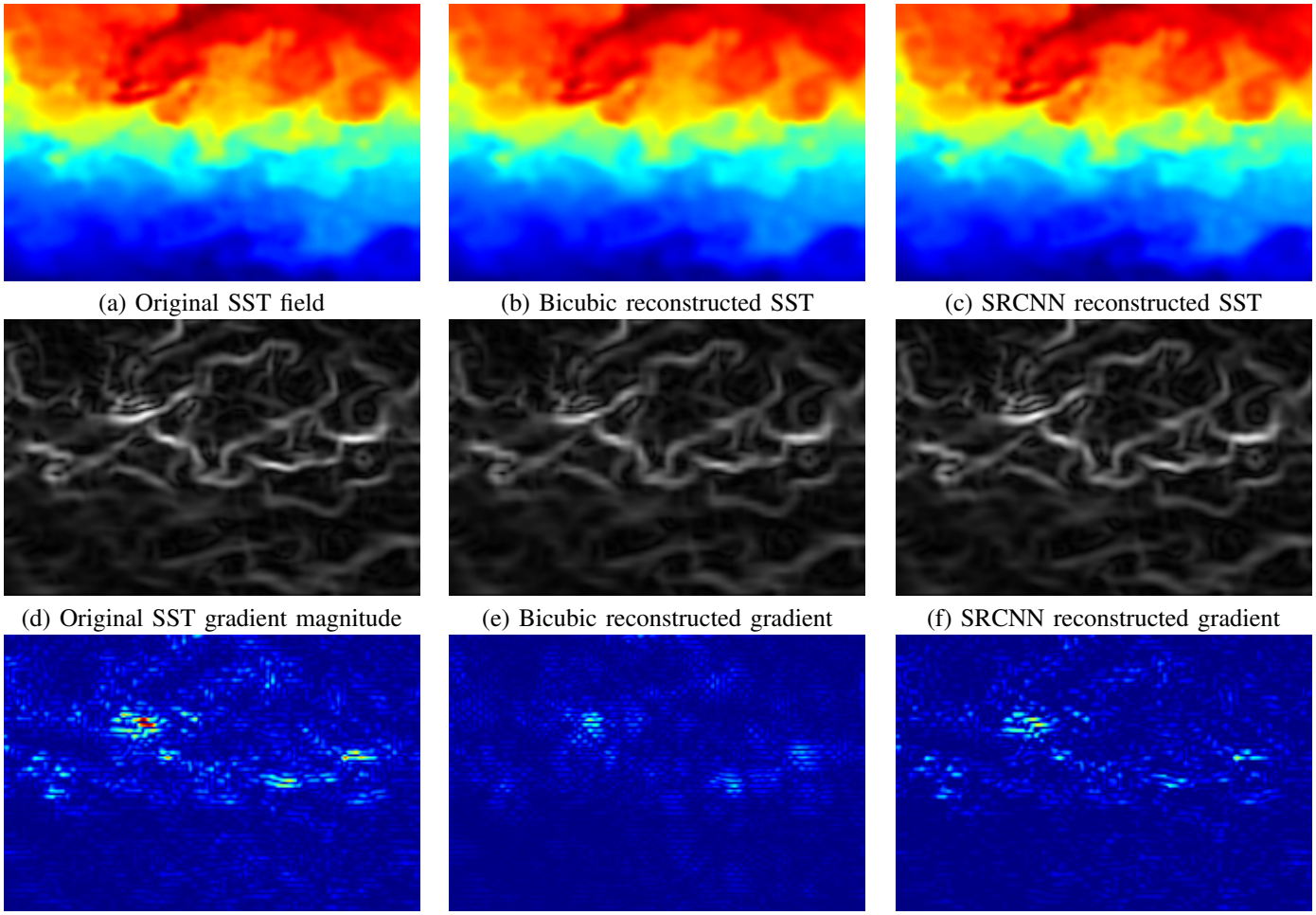

(a) Original SST field (b) Bicubic reconstructed SST (c) SRCNN reconstructed SST

(d) Original SST gradient magnitude (e) Bicubic reconstructed gradient (f) SRCNN reconstructed gradient

(g) Bicubic reconstruction residuals (h) SRCNN reconstruction residuals (i) Residuals gain (SRCNN vs. Bicubic)

Fig. 4. Top row: Original and reconstructed SST fields. Middle row: Original and reconstructed gradient magnitudes. Bottom row: residuals between original and reconstructed SST fields (g and h), and residuals difference between bicubic and SRCNN reconstructed SST fields (i).

[8] K. I. Kim and Y. Kwon, "Single-Image Super-Resolution Using Sparse Regression and Natural Image Prior," *IEEE Transactions on Pattern Analysis and Machine Intelligence*, vol. 32, no. 6, pp. 1127–1133, Jun. 2010.

[9] J. Yang, Z. Lin, and S. Cohen, "Fast Image Super-Resolution Based on In-Place Example Regression," in *2013 IEEE Conference on Computer Vision and Pattern Recognition (CVPR)*, Jun. 2013, pp. 1059–1066.

[10] J. B. Huang, A. Singh, and N. Ahuja, "Single image super-resolution from transformed self-exemplars," in *2015 IEEE Conference on Computer Vision and Pattern Recognition*, Jun. 2015, pp. 5197–5206.

[11] H. Chang, D.-Y. Yeung, and Y. Xiong, "Super-resolution through neighbor embedding," in *2004 IEEE Conference on Computer Vision and Pattern Recognition*, vol. 1, Jun. 2004, pp. I–I.

[12] S. Schulter, C. Leistner, and H. Bischof, "Fast and accurate image upscaling with super-resolution forests," in *2015 IEEE Conference on Computer Vision and Pattern Recognition*, Jun. 2015, pp. 3791–3799.

[13] J. Yang, J. Wright, T. S. Huang, and Y. Ma, "Image Super-Resolution Via Sparse Representation," *IEEE Transactions on Image Processing*, vol. 19, no. 11, pp. 2861–2873, Nov. 2010.

[14] R. Timofte, V. DeSmet, and L. VanGool, "A+: Adjusted Anchored Neighborhood Regression for Fast Super-Resolution," in *Computer Vision – ACCV 2014*, ser. Lecture Notes in Computer Science. Springer International Publishing, Nov. 2014, no. 9006, pp. 111–126.

[15] S. Gu, W. Zuo, Q. Xie, D. Meng, X. Feng, and L. Zhang, "Convolutional Sparse Coding for Image Super-Resolution," in *Proceedings of the IEEE International Conference on Computer Vision*, 2015, pp. 1823–1831.

[16] C. Dong, C. C. Loy, K. He, and X. Tang, "Image Super-Resolution Using Deep Convolutional Networks," *IEEE Transactions on Pattern Analysis and Machine Intelligence*, vol. 38, no. 2, pp. 295–307, Feb. 2016.

[17] J. Kim, J. K. Lee, and K. M. Lee, "Accurate Image Super-Resolution Using Very Deep Convolutional Networks," *arXiv:1511.04587 [cs]*, Nov. 2015, arXiv: 1511.04587.

[18] ——, "Deeply-Recursive Convolutional Network for Image Super-Resolution," *arXiv:1511.04491 [cs]*, Nov. 2015, arXiv: 1511.04491.

[19] J. Xie, L. Xu, and E. Chen, "Image Denoising and Inpainting with Deep Neural Networks," in *Advances in Neural Information Processing Systems*, 2012, pp. 350–358.

[20] L. A. Gatys, A. S. Ecker, and M. Bethge, "Texture Synthesis Using Convolutional Neural Networks," in *Advances in Neural Information Processing Systems 28*, 2015.

[21] C. J. Donlon, M. Martin, J. Stark, J. Roberts-Jones, E. Fiedler, and W. Wimmer, "The Operational Sea Surface Temperature and Sea Ice Analysis (OSTIA) system," *Remote Sensing of Environment*, vol. 116, pp. 140–158, Jan. 2012.

[22] Y. LeCun, Y. Bengio, and G. Hinton, "Deep learning," *Nature*, vol. 521, no. 7553, pp. 436–444, May 2015.

[23] J. Deng, W. Dong, R. Socher, L. J. Li, K. Li, and L. Fei-Fei, "ImageNet: A large-scale hierarchical image database," in *IEEE Conference on Computer Vision and Pattern Recognition*, Jun. 2009, pp. 248–255.

[24] Y. Jia, E. Shelhamer, J. Donahue, S. Karayev, J. Long, R. Girshick, S. Guadarrama, and T. Darrell, "Caffe: Convolutional Architecture for Fast Feature Embedding." ACM Press, 2014, pp. 675–678.